Supplement of Geosci. Model Dev., 15, 3079–3120, 2022
https://doi.org/10.5194/gmd-15-3079-2022-supplement

Geoscientific Model Development
Open Access

Supplement of

Multiphase processes in the EC-Earth model and their relevance to the atmospheric oxalate, sulfate, and iron cycles

Stelios Myriokefalitakis et al.

Correspondence to: Stelios Myriokefalitakis (steliosm@noa.gr)

Supplementary Tables

Table S1: Averaged factors for the years 2000-2014 used to represent the Fe-containing aerosols in the emitted fine and coarse aerosols of the model, as applied to a) the calculated dust mineral emissions as derived from the updated mineralogy maps originally created by Claquin et al. (1999), b) the CMIP6 anthropogenic emission sectors (Hoesly et al., 2018) as retrieved based on estimates from Ito et al. (2018) for the emitted submicron carbonaceous particulate matter (i.e., sum of OC and BC) and inorganic matter, and c) the CMIP6 biomass burning emissions (van Marle et al., 2017) also based on Ito et al. (2018) estimates. In parentheses, the standard deviation (where available) is also provided.

Fe types	Fine aerosols	Coarse aerosols
a) Dust minerals		
Illite	0.048	
Smectite	0.164	
Kaolinite	0.007	
Feldspars	0.025	
Iron oxides	0.660	
b) Anthropogenic sectors		
Energy	$1.861 \bullet 10^{-2}$ ($\pm 6.281 \bullet 10^{-4}$)	$3.528 \bullet 10^{-1}$ ($\pm 1.190 \bullet 10^{-2}$)
Industrial	$1.459 \bullet 10^{-2}$ ($\pm 1.414 \bullet 10^{-3}$)	$2.764 \bullet 10^{-1}$ ($\pm 2.681 \bullet 10^{-2}$)
Residential & Commercial	$4.336 \bullet 10^{-6}$ ($\pm 3.485 \bullet 10^{-7}$)	$1.350 \bullet 10^{-5}$ ($\pm 1.085 \bullet 10^{-6}$)
Shipping	$3.751 \bullet 10^{-2}$ ($\pm 9.043 \bullet 10^{-9}$)	$1.398 \bullet 10^{-2}$ ($\pm 4.454 \bullet 10^{-9}$)
Waste treatment	$1.389 \bullet 10^{-3}$ ($\pm 9.622 \bullet 10^{-11}$)	$3.595 \bullet 10^{-3}$ ($\pm 8.487 \bullet 10^{-10}$)
c) Biomass Burning	$6.292 \bullet 10^{-3}$	$2.296 \bullet 10^{-2}$

Table S2. Aqueous phase chemical mechanism and reaction rate constants. The photolysis frequencies (J) are expressed in s^{-1}, and the aqueous reactions (K) are expressed in $L\ mol^{-1}\ s^{-1}$.

	Aqueous-phase Reactions			J_{max}/K_{298}	E_a/R	Reference
	Photolysis					
J01	$O_3 + h\nu\ (+ H_2O)$	→	$H_2O_2 + O_2$	[a]		
J02	$H_2O_2 + h\nu$	→	$2\ OH$	[a]		
J03	$NO_3 + h\nu$	→	$NO + O_2$	[a]		
J04	$NO_3 + h\nu$	→	$NO_2 + O_3$	[a]		
J05	$NO_2^- + h\nu\ (+ H^+)$	→	$NO + OH$	[a]		
J06	$NO_3^- + h\nu\ (+ H^+)$	→	$NO_2 + OH$	[a]		
J07	$CH_3O_2H + h\nu\ (+ O_2)$	→	$CH_2(OH)_2 + HO_2 + OH$	[a]		
J08	$Fe^{+3} + h\nu\ (+ H_2O)$	→	$Fe^{+2} + OH + H^+$	$6.41\ 10^{-6}$ [b]		Deguillaume et al. (2004)
J09	$[Fe(OH)]^{2+} + h\nu$	→	$Fe^{2+} + OH$	$5.63\ 10^{-3}$ [b]		Deguillaume et al. (2004)
J10	$[Fe(OH)_2]^+ + h\nu$	→	$Fe^{2+} + OH + HO^-$	$7.52\ 10^{-3}$ [b]		Deguillaume et al. (2004)
J11	$[Fe(SO_4)]^+ + h\nu\ (+ H_2O)$	→	$Fe^{2+} + SO_4^{2-} + OH + H^+$	$4.51\ 10^{-5}$ [b]		Deguillaume et al. (2004)
J12	$[Fe(OXL)_2]^- + h\nu\ (+ O_2)$	→	$Fe^{+2} + OXL^{2-} + O_2^- + 2\ CO_2$	$2.47\ 10^{-2}$ [b]		Ervens et al. (2003)
	H_xO_y chemistry					
K001	$O_3 + OH$	→	$HO_2 + O_2$	$1.1\ 10^{8}$		Deguillaume et al. (2010)
K002	$O_3 + HO_2$	→	$OH + 2\ O_2$	$1.0\ 10^{4}$		Deguillaume et al. (2010)
K003	$O_3 + O_2^-\ (+ H_2O)$	→	$OH + O_2 + HO^-$	$1.5\ 10^{9}$	2200	Deguillaume et al. (2010)
K004	$HO_2 + OH$	→	$O_2 + H_2O$	$1.0\ 10^{10}$		Ervens et al. (2003)
K005	$O_2^- + OH$	→	$O_2 + HO^-$	$1.1\ 10^{10}$	2120	Ervens et al. (2003)
K006	$HO_2 + HO_2$	→	$H_2O_2 + O_2$	$8.3\ 10^{5}$	2720	Ervens et al. (2003)
K007	$HO_2 + O_2^-\ (+ H^+)$	→	$H_2O_2 + O_2$	$9.7\ 10^{7}$	1060	Ervens et al. (2003)
K008	$OH + OH$	→	H_2O_2	$3.6\ 10^{9}$	930	Deguillaume et al. (2010)
K009	$H_2O_2 + OH$	→	$HO_2 + H_2O$	$3.0\ 10^{7}$	1680	Ervens et al. (2003)
	Nitrogen chemistry					
K010	$NO + OH$	→	$NO_2^- + H^+$	$2.2\ 10^{10}$	1500	Deguillaume et al. (2010)
K011	$NO_2 + NO\ (+ H_2O)$	→	$2\ NO^- + 2\ H^+$	$3.0\ 10^{8}$		Deguillaume et al. (2010)
K012	$NO_2 + NO_2\ (+ H_2O)$	→	$HONO + NO_3^- + H^+$	$8.4\ 10^{7}$	-2900	Ervens et al. (2003)
K013	$NO_2 + OH$	→	$NO_3^- + H^+$	$1.2\ 10^{10}$		Ervens et al. (2003)
K014	$NO_3 + HO_2$	→	$NO_3^- + O_2 + H^+$	$3.0\ 10^{9}$		Ervens et al. (2003)
K015	$NO_3 + O_2^-$	→	$NO_3^- + O_2$	$3.0\ 10^{9}$		Ervens et al. (2003)
K016	$NO_3 + H_2O_2$	→	$NO_3^- + HO_2 + H^+$	$4.9\ 10^{6}$	2000	Deguillaume et al. (2004)
K017	$NO_3 + HO^-$	→	$NO_3^- + OH$	$9.4\ 10^{7}$	2700	Ervens et al. (2003)
K018	$NO_2^- + O_3$	→	$NO_3^- + O_2$	$5.0\ 10^{5}$	7000	Ervens et al. (2003)
K019	$HONO + OH$	→	$NO_2 + H_2O$	$1.0\ 10^{10}$		Deguillaume et al. (2010)
K020	$NO_2^- + OH$		$NO_2 + HO^-$	$1.1\ 10^{10}$		Ervens et al. (2003)
K021	$NO_2^- + CO_3^-$	→	$NO_2 + CO_3^{2-}$	$6.6\ 10^{5}$	850	Ervens et al. (2003)
	Sulfur chemistry					
K022	$SO_2 + O_3\ (+ H_2O)$	→	$HSO_4^- + O_2 + H^+$	$2.4\ 10^{4}$		Seinfeld and Pandis (2006)
K023	$HSO_3^- + O_3$	→	$HSO_4^- + O_2$	$3.7\ 10^{5}$	5530	Seinfeld and Pandis (2006)
K024	$SO_3^{2-} + O_3$	→	$SO_4^{2-} + O_2$	$1.5\ 10^{9}$	5280	Seinfeld and Pandis (2006)
K025	$HSO_3^- + H_2O_2\ (+ H^+)$	→	$H_2SO_4 + H_2O$	[$]		Seinfeld and Pandis (2006)
K026	$SO_2 + HO_2\ (+ H_2O)$	→	$H_2SO_4 + OH$	$1.0\ 10^{6}$		Seinfeld and Pandis (2006)
K027	$SO_2 + O_2^-\ (+ H_2O)$	→	$HSO_3^- + OH + HO^-$	$1.0\ 10^{5}$		Seinfeld and Pandis (2006)
K028	$HSO_3^- + CH_3O_2H\ (+ H^+)$	→	$SO_4^{2-} + CH_3OH + 2H^+$	$1.7\ 10^{7}$	3160	Seinfeld and Pandis (2006)
	Carbonate chemistry					
K029	$HCO_3^- + OH$	→	$CO_3^- + H_2O$	$1.7\ 10^{7}$	1900	Ervens et al. (2003)
K039	$CO_3^{2-} + OH$	→	$CO_3^- + HO^-$	$3.9\ 10^{8}$	2840	Ervens et al. (2003)
K031	$HCO_3^- + NO_3$	→	$CO_3^- + NO_3^- + H^+$	$4.1\ 10^{7}$		Ervens et al. (2003)
K032	$CO_3^{2-} + NO_3$	→	$CO_3^- + NO_3^-$	$4.1\ 10^{7}$		Ervens et al. (2003)
K033	$CO_3^- + O_3$	→	$CO_2 + O_2^- + O_2$	$1.0\ 10^{5}$		Ervens et al. (2003)

K034	$CO_3^- + HO_2$	→	$HCO_3^- + O_2$	$6.5\ 10^8$		Ervens et al. (2003)
K035	$CO_3^- + O_2^-$	→	$CO_3^{2-} + O_2$	$6.5\ 10^8$		Ervens et al. (2003)
K036	$CO_3^- + H_2O_2$	→	$HCO_3^- + HO_2$	$4.3\ 10^5$		Ervens et al. (2003)
K037	$CO_3^- + NO_2$	→	$CO_2 + NO_3^-$	$1.0\ 10^9$		Ervens et al. (2003)
K038	$CO_3^- + CO_3^-$ (+ O_2)	→	2 O_2^- + 2 CO_2	$2.2\ 10^6$		Ervens et al. (2003)
	Organic chemistry					
K039	CH_3O_2H + OH	→	0.8 (CH_3O_2 + H_2O) + 0.2 (HCOOH + HO_2)	$3.0\ 10^7$	1680	Ervens et al. (2003)
K040	$CH_3O_2H + CO_3^-$	→	$CH_3O_2 + HCO_3^-$	$4.3\ 10^5$		Ervens et al. (2003)
K041	$CH_3O_2 + HO_2$	→	$CH_3O_2H + O_2$	$4.2\ 10^5$	3000	Deguillaume et al. (2010)
K042	$CH_3O_2 + O_2^-$ (+ H_2O)	→	$CH_3O_2H + O_2 + HO^-$	$4.8\ 10^7$	1600	Deguillaume et al. (2010)
K043	$CH_3O_2 + CH_3O_2$ (+ H_2O)	→	$CH_3OH + CH_2(OH)_2 + O_2$	$1.7\ 10^8$	2200	Ervens et al. (2003)
K044	$CH_3O_2 + CH_3O_2$ (+ 2 O_2 + 2 H_2O)	→	2 $CH_2(OH)_2$ + 2 HO_2 + O_2	$3.6\ 10^7$	2200	Ervens et al. (2003)
K045	$CH_2(OH)_2$ + OH (+ O_2)	→	HCOOH + HO_2 + H_2O	$1.0\ 10^9$	1020	Ervens et al. (2003)
K046	$CH_2(OH)_2 + NO_3$ (+ O_2)	→	HCOOH + $HO_2 + NO_3^- + H^+$	$1.0\ 10^6$	4500	Ervens et al. (2003)
K047	CH_3OH + OH (+ O_2)	→	$CH_2(OH)_2 + HO_2 + H_2O$	$1.0\ 10^9$	580	Ervens et al. (2003)
K048	$CH_3OH + NO_3$ (+ O_2)	→	$CH_2(OH)_2 + HO_2 + NO_3^-$	$5.4\ 10^5$	4300	Ervens et al. (2003)
K049	$CH_3OH + CO_3^-$ (+ O_2)	→	$CH_2(OH)_2 + HO_2 + HCO_3^-$	$2.6\ 10^3$		Ervens et al. (2003)
K050	HCOOH + OH (+ O_2)	→	$CO_2 + HO_2 + H_2O$	$1.3\ 10^8$	1000	Ervens et al. (2003)
K051	$HCOO^-$ + OH (+ O_2)	→	$CO_2 + HO_2 + HO^-$	$3.2\ 10^9$	1000	Ervens et al. (2003)
K052	HCOOH + NO_3 (+ O_2)	→	$CO_2 + HO_2 + NO_3^- + H^+$	$3.8\ 10^5$	3400	Ervens et al. (2003)
K053	$HCOO^- + NO_3$ (+ O_2)	→	$CO_2 + HO_2 + NO_3^-$	$5.1\ 10^7$	2200	Ervens et al. (2003)
K054	$HCOO^- + CO_3^-$ (+ O_2)	→	2 $CO_2 + O_2^- + HO^-$	$1.4\ 10^5$	3300	Ervens et al. (2003)
K055	$CH_3CH(OH)_2$ + OH (+ O_2)	→	$CH_3COOH + HO_2 + H_2O$	$1.2\ 10^9$		Ervens et al. (2003)
K056	$CH_3CH(OH)_2 + NO_3$ (+ O_2)	→	$CH_3COOH + HO_2 + NO_3^- + H^+$	$1.9\ 10^6$		Ervens et al. (2003)
K057	$CH_3CH(OH)_2 + CO_3^-$ (+ O_2)	→	$CH_3COOH + HO_2 + CO_2$	$1.0\ 10^4$		Ervens et al. (2003)
K058	GLYAL + OH (+ O_2)	→	GLY + HO_2	$1.0\ 10^9$		Lim et al. (2005)
K059	GLYAL + OH (+ O_2)	→	GLX + 2 HO_2	$5.0\ 10^8$		Lim et al. (2005)
K060	GLYAL + NO_3 (+ O_2)	→	GLY + $HO_2 + NO_3^- + H^+$	$1.1\ 10^7$		Herrmann et al. (2005)
K061	GLYAL + NO_3 (+ O_2)	→	GLX + 2 $HO_2 + NO_3^- + H^+ + H_2O$	$5.5\ 10^6$		Herrmann et al. (2005)
K062	GLY + OH (+ O_2)	→	GLX + HO_2 + H_2O	$1.1\ 10^9$	1516	Ervens et al. (2003)
K063	GLY + OH	→	GLYOLIG [c]	$3.0\ 10^{10}$		Carlton et al. (2007)
K064	GLYOLIG [c] + OH	→	OXL	$3.0\ 10^{10}$		Carlton et al. (2007)
K065	GLYOLIG [c] + OH	→	GLX	$1.0\ 10^9$		Carlton et al. (2007)
K066	GLY + NO_3 (+ O_2)	→	GLX + $HO_2 + NO_3^- + H^+$	$1.1\ 10^6$	3368	Ervens et al. (2003)
K067	CH_3CH_2OH + OH (+ O_2)	→	$CH_3CH(OH)_2 + HO_2$	$1.9\ 10^9$		Ervens et al. (2003)
K068	$CH_3CH_2OH + NO_3$ (+ O_2)	→	$CH_3CH(OH)_2 + HO_2 + NO_3^- + H^+$	$2.2\ 10^6$		Ervens et al. (2003)
K069	$CH_3CH_2OH + CO_3^-$ (+ O_2)	→	$CH_3CH(OH)_2 + HO_2 + CO_2$	$1.5\ 10^4$		Ervens et al. (2003)
K070	CH_3COOH + OH (+ O_2)	→	0.85 GLX + 0.15 $CH_2(OH)_2$ + 0.15 CO_2 + HO_2	$1.5\ 10^7$	1330	Ervens et al. (2003)
K071	CH_3COO^- + OH (+ O_2)	→	0.85 GLX^- + 0.15 $CH_2(OH)_2$ + 0.15 CO_2 + HO_2	$1.0\ 10^8$	1800	Ervens et al. (2003)
K072	$CH_3COOH + NO_3$ (+ O_2)	→	0.85 GLX^- + 0.15 $CH_2(OH)_2$ + 0.15 $CO_2 + NO_3^- + H^+$	$1.4\ 10^4$	3800	Ervens et al. (2003)
K073	$CH_3COO^- + NO_3$ (+ O_2)	→	0.85 GLX^- + 0.15 $CH_2(OH)_2$ + 0.15 $CO_2 + NO_3^- + H^+$	$2.9\ 10^6$	3800	Ervens et al. (2003)
K074	$CH_3COO^- + CO_3^-$ (+ O_2)	→	0.85 GLX^- + 0.15 $CH_2(OH)_2$ + 1.15 CO_2	$5.8\ 10^2$		Ervens et al. (2003)
K075	HYAC + OH	→	MGLY + HO_2	$1.2\ 10^9$		Herrmann et al. (2005)
K076	HYAC + NO_3	→	MGLY + $NO_3^- + H^+$	$1.7\ 10^6$		Herrmann et al. (2005)
K077	MGLY + OH (+ O_2)	→	0.92 PRV + 0.08 GLX + 0.08 CO_2 + HO_2 + H_2O	$1.1\ 10^9$	1600	Ervens et al. (2004)
K078	MGLY + OH	→	0.8 MGLYOLIG [c] + 0.2 OXL	$1.1\ 10^9$	1600	Lin et al. (2014) (Tan et al., 2012)
K079	MGLY + NO_3 (+ O_2)	→	0.92 PRV + 0.08 GLX + 0.08 $CO_2 + HO_2 + NO_3^- + H^+$	$6.3\ 10^7$		Herrmann et al. (2005)
K080	PRV + OH (+ O_2)	→	$CH_3COOH + HO_2 + CO_2$	$1.2\ 10^8$	2800	Herrmann et al. (2005)
K081	PRV^- + OH	→	$CH_3COO^- + HO_2 + CO_2$	$7.0\ 10^8$	2285	Herrmann et al. (2005)
K082	PRV + NO_3 (+ O_2 + H_2O)	→	$CH_3COOH + CO_2 + HO_2 + NO_3^- + H^+$	$4.8\ 10^6$		Herrmann et al. (2005)
K083	$PRV^- + NO_3$ (+ O_2 + H_2O)	→	$CH_3COO^- + CO_2 + HO_2 + NO_3^- + H^+$	$1.9\ 10^8$		Herrmann et al. (2005)
K084	GLX + OH (+ O_2)	→	OXL + HO_2 + H_2O	$3.6\ 10^8$	1000	Deguillaume et al. (2009)
K085	GLX^- + OH (+ O_2)	→	OXL^- + HO_2 + H_2O	$2.6\ 10^9$	4330	Deguillaume et al. (2009)
K086	GLX + NO_3 (+ O_2)	→	OXL + $HO_2 + NO_3^- + H^+$	$3.0\ 10^6$		as for glycolic acid from Herrmann et al. (2005)
K087	$GLX^- + NO_3$ (+ O_2)	→	$OXL^- + HO_2 + NO_3^- + H^+$	$1.1\ 10^8$		as for glycolic acid from Herrmann et al. (2005)
K088	OXL^- + OH (+ O_2)	→	$2CO_2 + HO_2 + H_2O$	$1.4\ 10^6$		Ervens et al. (2004)
K089	OXL^- + OH (+ O_2)	→	$2CO_2 + O_2^- + H_2O$	$3.2\ 10^7$		Ervens et al. (2003)
K090	OXL^{2-} + OH (+ O_2)	→	$2CO_2 + O_2^- + HO^-$	$5.3\ 10^6$		Ervens et al. (2003)
K091	OXL + NO_3 (+ O_2)	→	$2CO_2 + NO_3^- + H^+ + HO_2$	$6.8\ 10^7$		
K092	$OXL^- + NO_3$ (+ O_2)	→	$2CO_2 + NO_3^- + H^+ + O_2^-$	$6.8\ 10^7$		Ervens et al. (2003)
K093	$OXL^{2-} + NO_3$ (+ O_2)	→	$2CO_2 + NO_3^- + O_2^-$	$2.2\ 10^8$		Ervens et al. (2003)
	Iron chemistry					
K094	$Fe^{3+} + O_2^-$	→	$Fe^{2+} + O_2$	$1.5\ 10^8$		Ervens et al. (2003)
K095	$[Fe(OH)]^{2+} + HO_2$	→	$Fe^{2+} + O_2 + H_2O$	$1.3\ 10^5$		Ervens et al. (2003)
K096	$[Fe(OH)]^{2+} + O_2^-$	→	$Fe^{2+} + O_2 + HO^-$	$1.5\ 10^8$		Ervens et al. (2003)
K097	$Fe^{3+} + SO_4^{2-}$	→	$[Fe(SO_4)]^+$	$3.2\ 10^3$		Deguillaume et al. (2004)
K098	$[Fe(SO_4)]^+$	→	$Fe^{3+} + SO_4^{2-}$	$2.7\ 10^1$		Deguillaume et al. (2004)
K099	$[Fe(SO_4)]^+ + HO_2$	→	$Fe^{2+} + SO_4^{2-} + O_2 + H^+$	$1.0\ 10^5$		Deguillaume et al. (2004)
K100	$[Fe(SO_4)]^+ + O_2^-$	→	$Fe^{2+} + SO_4^{2-} + O_2$	$1.5\ 10^8$		Deguillaume et al. (2004)
K101	Fe^{2+} + OH	→	$[Fe(OH)]^{2+}$	$4.3\ 10^8$	1100	Ervens et al. (2003)
K102	$Fe^{2+} + HO_2$ (+ H^+)	→	$Fe^{3+} + H_2O_2$	$1.2\ 10^6$	5050	Ervens et al. (2003)
K103	$Fe^{2+} + O_2^-$ (+ $2H^+$)	→	$Fe^{3+} + H_2O_2$	$1.0\ 10^7$		Ervens et al. (2003)
K104	$Fe^{2+} + H_2O_2$	→	Fe^{3+} + OH + HO^-	$5.0\ 10^1$		Ervens et al. (2003)
K105	$Fe^{2+} + O_3$	→	$FeO^{2+} + O_2$	$8.2\ 10^5$		Ervens et al. (2003)
K106	$Fe^{2+} + NO_2$	→	$Fe^{3+} + NO_2^-$	$3.1\ 10^4$		Deguillaume et al. (2004)
K107	$Fe^{2+} + NO_3$	→	$Fe^{3+} + NO_3^-$	$8.0\ 10^6$		Deguillaume et al. (2004)
K108	$Fe^{2+} + CO_3^-$	→	$Fe^{3+} + CO_3^{2-}$	$2.7\ 10^7$		Ervens et al. (2003)
K109	$Fe^{2+} + CH_3O_2$	→	$Fe^{3+} + CH_3O_2H + HO^-$	$8.6\ 10^5$		Ervens et al. (2003)
K110	FeO^{2+} + OH (+ H^+)	→	$Fe^{3+} + H_2O_2$	$1.0\ 10^7$		Ervens et al. (2003)
K111	$FeO^{2+} + HO_2$	→	$Fe^{3+} + O_2 + HO^-$	$2.0\ 10^6$		Ervens et al. (2003)
K112	$FeO^{2+} + H_2O_2$	→	$Fe^{3+} + HO_2 + HO^-$	$9.5\ 10^3$	2766	Ervens et al. (2003)
K113	$FeO^{2+} + H_2O$	→	Fe^{3+} + OH + HO^-	$2.34\ 10^{-4}$	4089	Ervens et al. (2003)
K114	$FeO^{2+} + Fe^{2+}$ (+ H_2O)	→	2 Fe^{3+} + 2 HO^-	$1.8\ 10^4$	5052	Ervens et al. (2003)
K115	FeO^{2+} + HONO	→	$Fe^{3+} + NO_2 + HO^-$	$1.1\ 10^4$	4150	Ervens et al. (2003)
K116	$FeO^{2+} + NO_2^-$ (+ H^+)	→	$Fe^{3+} + NO_2 + HO^-$	$1.0\ 10^5$		Ervens et al. (2003)
K117	$FeO^{2+} + CH_2(OH)_2$ (+ O_2)	→	Fe^{3+} + HCOOH + $HO_2 + HO^-$	$4.0\ 10^2$	5352	Ervens et al. (2003)
K118	FeO^{2+} + HCOOH (+ O_2 + H^+)	→	$Fe^{3+} + HO_2 + CO_2 + H_2O$	$1.6\ 10^1$	2680	Ervens et al. (2003)
K119	$FeO^{2+} + HCOO^-$ (+ O_2)	→	$Fe^{3+} + O_2^- + CO_2 + HO^-$	$3.0\ 10^5$		Ervens et al. (2003)
K120	$Fe^{3+} + OXL^{2-}$	→	$[Fe(OXL)]^+$	$7.5\ 10^6$		Ervens et al. (2003)
K121	$[Fe(OXL)]^+$	→	$Fe^{3+} + OXL^{2-}$	$3.0\ 10^{-3}$		Ervens et al. (2003)
K122	$[Fe(OXL)]^+ + OXL^{2-}$	→	$[Fe(OXL)_2]^-$	$1.89\ 10^4$		Ervens et al. (2003)
K123	$[Fe(OXL)_2]^-$	→	$[Fe(OXL)]^+ + OXL^{2-}$	$3.0\ 10^{-3}$		Ervens et al. (2003)
K124	$[Fe(OXL)]^+ + HO_2$	→	$Fe(OXL) + O_2 + H^+$	$1.2\ 10^5$		Sedlak and Hoigné (1993)
K125	$[Fe(OXL)]^+ + O_2^-$	→	$Fe(OXL) + O_2$	$1.0\ 10^6$		Sedlak and Hoigné (1993)

K126	Fe(OXL) + H_2O_2	→	$[Fe(OXL)]^+$ + OH + HO^-	3.1 10^4	Sedlak and Hoigné (1993)
K127	Fe^{2+} + OXL^{2-}	→	Fe(OXL)	3.67 10^5	Sedlak and Hoigné (1993)
K128	Fe(OXL)	→	Fe^{2+} + OXL^{2-}	3.0 10^{-3}	as for K121 and K123

a) using the calculated gas-phase photolysis frequencies.
b) aqueous-phase photolysis rates at noontime scaled on model's H_2O_2 gas-phase photolysis frequencies.
c) representing large multifunctional compounds (see Carlton et al., 2007).

Table S3: Henry's law solubility constants (H), mass accommodation coefficients (α) and gas phase diffusion coefficients (Dg) used in aqueous-phase chemistry scheme.

Trace gas	H (mol m^{-3} Pa^{-1})	-ΔH R^{-1} (K)	Reference	α	Reference	D_g (m^2 s^{-1})	Reference
O_3	1.0 10^{-4}	2800	1	0.05	2	1.48 10^{-5}	2
H_2O_2	9.1 10^2	6600	1	0.11	2	1.46 10^{-5}	2
HO_2	6.8		1	0.01	2	1.04 10^{-5}	2
OH	3.8 10^{-1}		1	0.05	2	1.53 10^{-5}	2
NO	1.9 10^{-5}	1600	1	as for NO_2	2	as for NO_2	
NO_2	9.9 10^{-5}		1	0.0015	2	1.92 10^{-5}	2
NO_3	3.8 10^{-4}		1	0.004	2	1.00 10^{-5}	2
HONO	4.8 10^{-1}	4800	1	0.5	2	1.30 10^{-5}	2
HNO_3	8.8 10^2		1	0.054	2	1.32 10^{-5}	2
SO_2	1.3 10^{-2}	2900	1	0.035	2	1.28 10^{-5}	2
CO_2	3.3 10^{-4}	2400	1	0.0002	2	1.55 10^{-5}	2
CH_3O_2	1.5 10^{-1}	3700	1	as for CH_3O_2H	2	as for CH_3O_2H	2
CH_3O_2H	2.9	5200	1	0.0038	2	1.31 10^{-5}	2
HCHO	3.2 10^{-1}	6800	1	0.02	2	1.64 10^{-5}	2
CH_3OH	2.0	5600	1	0.015	2	1.16 10^{-5}	2
HCOOH	8.8 10^1	6100	1	0.012	2	1.53 10^{-5}	2
GLYAL	4.1 10^2	4600	1	as for GLY		as for GLY	
GLY	4.1 10^3	7500	1	0.023	3	1.15 10^{-5}	3
MGLY	3.4 10^1	7500	1	as for GLY		as for GLY	
HYAC	7.7 10^1		1	0.0176	4	9.50 10^{-7}	4
CH_3CHO	1.3 10^{-1}	5900	1	0.03	2	1.22 10^{-5}	2
CH_3CH_2OH	1.9	6400	1	0.0082	2	9.50 10^{-6}	2
CH_3COOH	4.0 10^1	6200	1	0.019	3	1.24 10^{-5}	2
PRV	3.1 10^3	5100	1	as for CH_3COOH		as for CH_3COOH	
GLX	1.1 10^2	4800	1	as for CH_3COOH		as for CH_3COOH	
H_2OXL	3.1 10^4	7300	1	as for CH_3COOH		as for CH_3COOH	

1) Sander (2015) and references therein.
2) Herrmann et al. (2000) and references therein.
3) Lim et al. (2005) and references therein.
4) Ervens et al. (2003) and references therein.

Table S4. Dissolution scheme for iron-containing combustion and mineral dust aerosols.

	Iron pool	Scheme [g]	K_{298} [a]	m [b]	K_{eq} [c]	n [d]	Reference
D01	Combustion Fe [e]	H^+	5.24 10^{-8}	0.36			Ito (2015)
D02		OXL	3.85 10^{-6}	1			Ito (2015)
D03		$h\nu^f$	4.10 10^{-6}	1			Ito (2015)
D04	Ferrihydrite	H^+	7.13 10^{-5}	1.1	1550	3	Ito and Shi (2016)
D05		OXL	4.61 10^{-8}	0.069	1550	3	Ito and Shi (2016)
D06		$h\nu^f$	4.61 10^{-8}	0.069			Ito and Shi (2016)
D07	Nano-Fe oxides	H^+	1.43 10^{-4}	1.6	42	2.75	Ito and Shi (2016)
D08		OXL	1.28 10^{-8}	0.069	1550	3	Ito and Shi (2016)
D09		$h\nu^f$	1.28 10^{-8}	0.069			Ito and Shi (2016)
D10	Aluminosilicates	H^+	5.85 10^{-8}	0.76	3.3	2.85	Ito and Shi (2016)
D11		OXL	1.68 10^{-9}	0.056	1500	3	Ito and Shi (2016)
D12		$h\nu^f$	1.68 10^{-9}	0.056			Ito and Shi (2016)

a) The dissolution rate constants (K) for combustion and mineral dust aerosols are expressed in mol Fe g^{-1} s^{-1} and defined as:

$$K = K_{228} \cdot exp\left[E_{pH} \cdot (1/298 - 1/T)\right]$$

where, E_{pH} = -1.56 10^3 · pH + 1.08 10^4 (Bibi et al., 2014; Ito and Shi, 2016)
b) m is the reaction order (Ito, 2015; Ito and Shi, 2016)
c) K_{eq} is the equilibrium constant (mol ^{2} kg^{-2}) (Bonneville et al., 2004; Ito and Shi, 2016)
d) n is the stoichiometric ratio (Bonneville et al., 2004; Ito and Shi, 2016).
e) The unit for combustion aerosol is converted from moles m^{-2} s^{-1} to mol Fe g^{-1} s^{-1} (Ito, 2015)
f) Photoinduced dissolution rate constants are scaled on the model's H_2O_2 gas-phase photolysis frequencies.
g) For the proton-promoted dissolution, suppressions are taken into account when the solution becomes supersaturated with respect to Fe(III), but any suppression due to OXL is neglected (i.e., $0 \le f_i \le 1$ and $g_i = 1$). For oxalate-promoted dissolution, the formation of amorphous $Fe(OH)_3$(s) (Shi et al., 2009, 2015) is assumed to inhibit the adsorption of OXL and, thus, the Fe release from the minerals' surface (i.e., $0 \le f_i \le 1$ and $0 \le g_i \le 1$). For combustion aerosols, both the OXL-promoted and photo-induced dissolution rates are also considered to be suppressed by the formation of amorphous $Fe(OH)_3$(s) (Ito, 2015).

Table S5: Aqueous phase equilibrium constants (E_k) used in aqueous-phase chemistry scheme.

Equilibrium Reaction			Ek_{298} (mol L^{-1})	$-\Delta H R^{-1}$ (K)	Reference
H_2O	↔	$HO^- + H^+$	$1.0\ 10^{-14}$	-6710	1
H_2O_2	↔	$HO_2^- + H^+$	$2.2\ 10^{-12}$	-3730	1
HO_2	↔	$O_2^- + H^+$	$3.5\ 10^{-5}$		1
CO_2 (+ H_2O)	↔	H_2CO_3	$7.7\ 10^{-7}$	-750	2
H_2CO_3	↔	$HCO_3^- + H^+$	$2.0\ 10^{-4}$		2
HCO_3^-	↔	$CO_3^{2-} + H^+$	$4.69\ 10^{-11}$	-1820	2
NH_4OH	↔	$NH_4^+ + HO^-$	$1.7\ 10^{-5}$	-450	1
$SO_2 \cdot H_2O$	↔	$HSO_3^- + H^+$	$1.3\ 10^{-2}$	1960	1
HSO_3^-	↔	$SO_4^{2-} + H^+$	$6.6\ 10^{-8}$	1500	1
HONO	↔	$NO_2^- + H^+$	$5.1\ 10^{-4}$	-1260	1
HNO_3	↔	$NO_3^- + H^+$	15.4	8700	1
HCOOH	↔	$HCOO^- + H^+$	$1.77\ 10^{-4}$	-12	3
CH_3COOH	↔	$CH_3COO^- + H^+$	$1.75\ 10^{-5}$	-46	3
PRV	↔	$PRV^- + H^+$	$3.2\ 10^{-3}$		4
GLX	↔	$GLX^- + H^+$	$3.47\ 10^{-4}$	-267	4
H_2OXL	↔	$HOXL^- + H^+$	$5.6\ 10^{-2}$	-453	4
$HOXL^-$	↔	$OXL^= + H^+$	$5.42\ 10^{-5}$	-805	4
Fe^{3+} (+ H_2O)	↔	$[Fe(OH)]^{2+} + H^+$	$1.1\ 10^{-4}$		3
$[Fe(OH)]^{2+}$ (+ H_2O)	↔	$[Fe(OH)_2]^+ + H^+$	$1.4\ 10^{-7}$		3

1) Seinfeld and Pandis (2006) and references therein.
2) Herrmann et al. (2000) and references therein.
3) Ervens et al. (2003) and references therein.
4) Lim et al. (2005) and references therein.

Supplementary Equations

Mathematical formulas for correlation coefficient (R; Eq. S1), normalized mean bias (nMB; Eq. S2), and the normalized root mean square error (nRMSE; Eq. S3), used for the statistical analysis of model comparison against observations; *O_i* and *P_i* stand for observations and predictions, respectively. N is the number of pairs (observations, predictions) that are compared.

$$R = \left[\frac{\frac{1}{N}\sum_{i=1}^{N}\left(O_i - \overline{O}\right)\left(P_i - \overline{P}\right)}{\sigma_O \sigma_P} \right] \quad \text{(Eq. S1)}$$

$$NMB = \frac{\sum_{i=1}^{N}\left(M_i - O_i\right)}{\sum_{i=1}^{N} O_i} \times 100 \quad \text{(Eq. S2)}$$

$$nRMSE = \frac{\sqrt{\frac{1}{N}\sum_{i=1}^{N}(P_i - O_i)^2}}{\sum_{i=1}^{N} O_i} \quad \text{(Eq. S3)}$$

Supplementary Figures

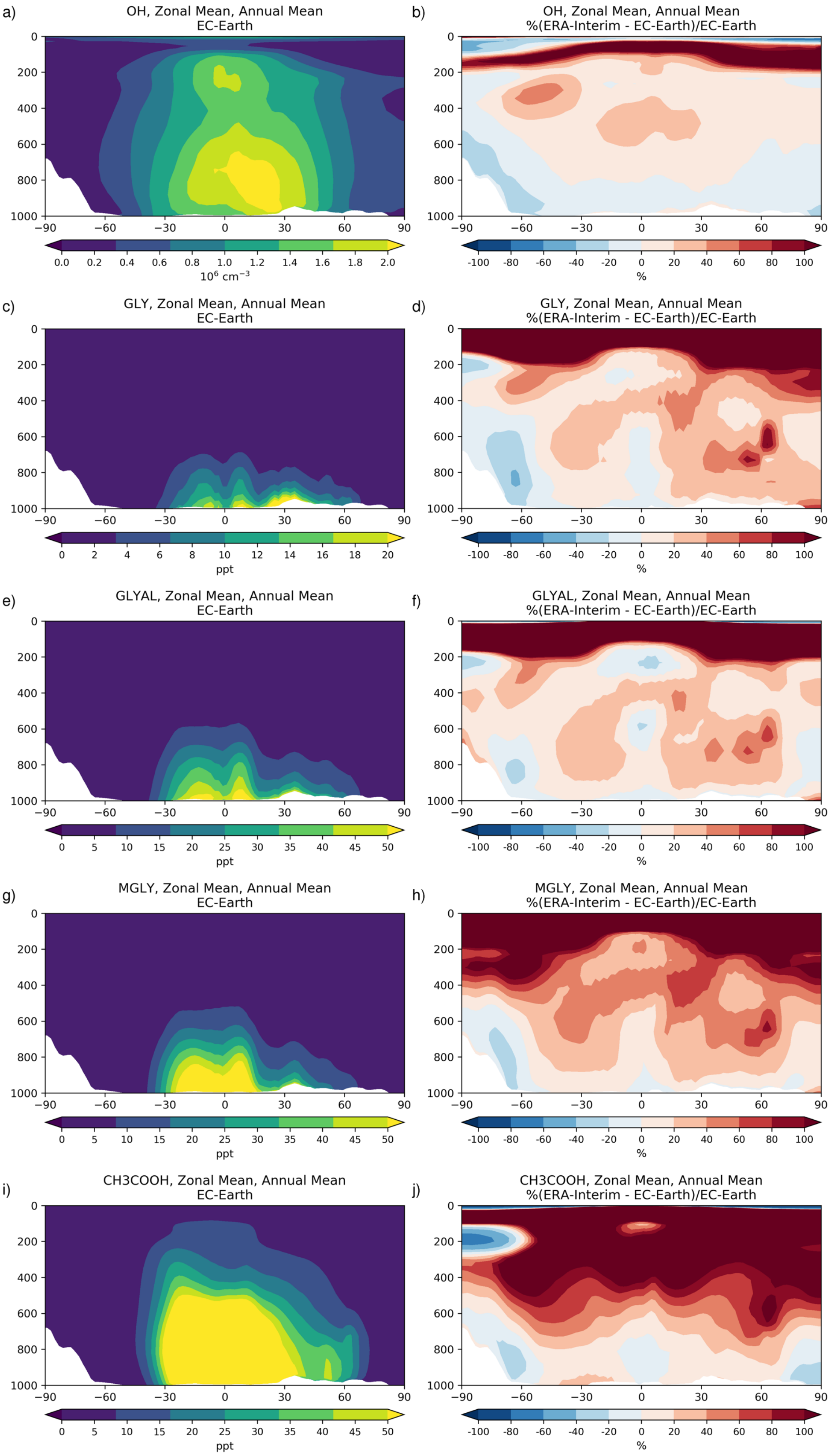

Figure S1: Annual mean zonal mean concentrations of a) OH radicals (10^6 molec. cm^{-3}), c) glyoxal (ppt), e) glycolaldehyde (ppt), g) methylglyoxal (ppt), and i) acetic acid (ppt), as simulated for the EC-Earth simulation, averaged for the period 2000-2014, and the absolute differences to the ERA-Interim simulation (b,d,f,h,j).

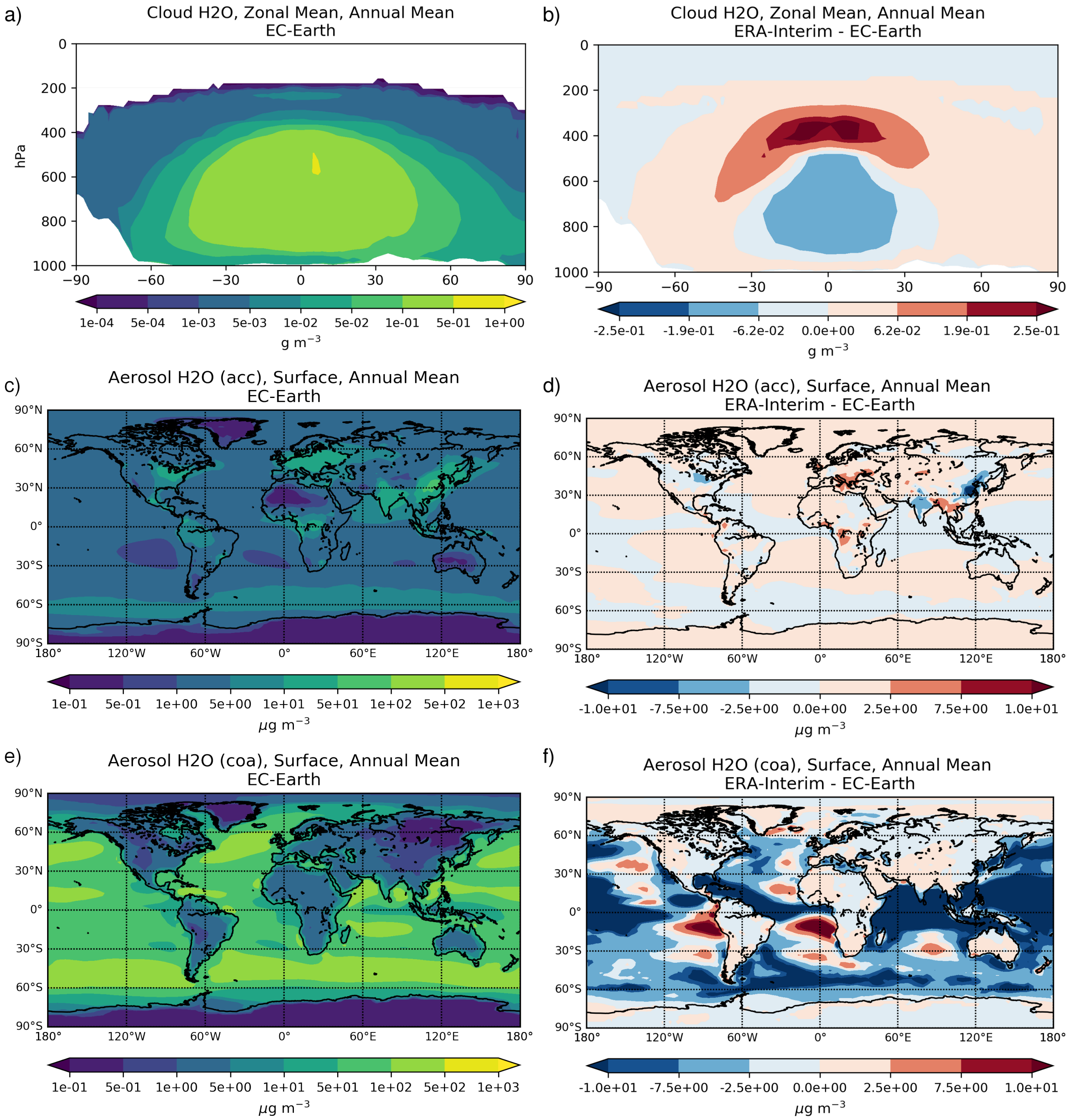

Figure S2: Annual mean of a) zonal mean concentrations of cloud water (g m^{-3}), c) surface concentrations of aerosol water associated with accumulation aerosols (μg m^{-3}), and e) surface concentrations of aerosol water associated with coarse aerosols (μg m^{-3}), as simulated for the EC-Earth simulation, averaged for the period 2000-2014, and the respective absolute differences to the ERA-Interim simulation (b,d,f).

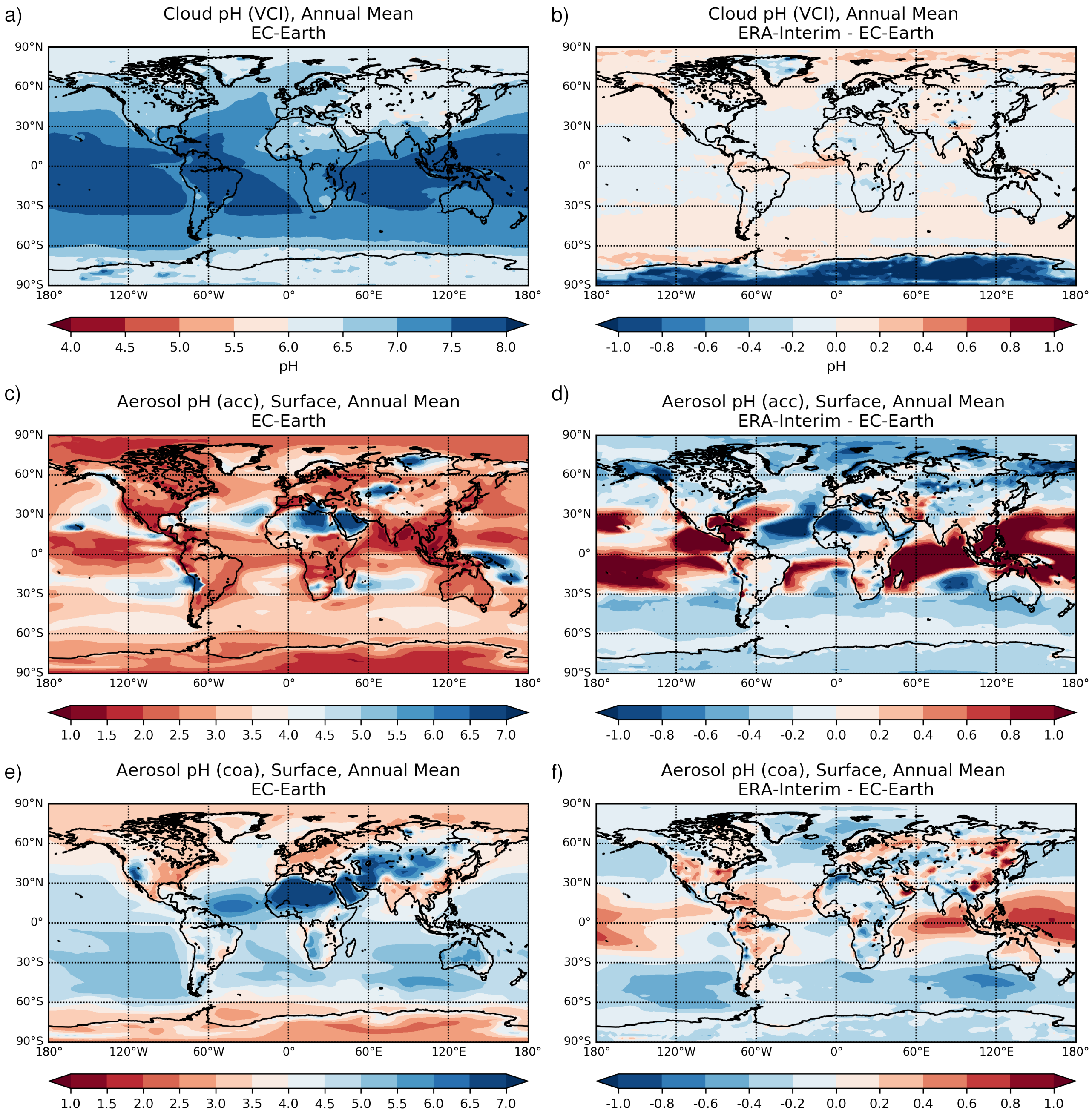

Figure S3: Annual mean a) vertical-column-integrated (VCI) liquid-water-weighted cloud water pH, c) accumulation aerosol pH at the surface, e) and coarse aerosol pH at the surface, as calculated for the EC-Earth simulation, averaged for the period 2000-2014, and the respective absolute differences to the ERA-Interim simulation (b,d,f).

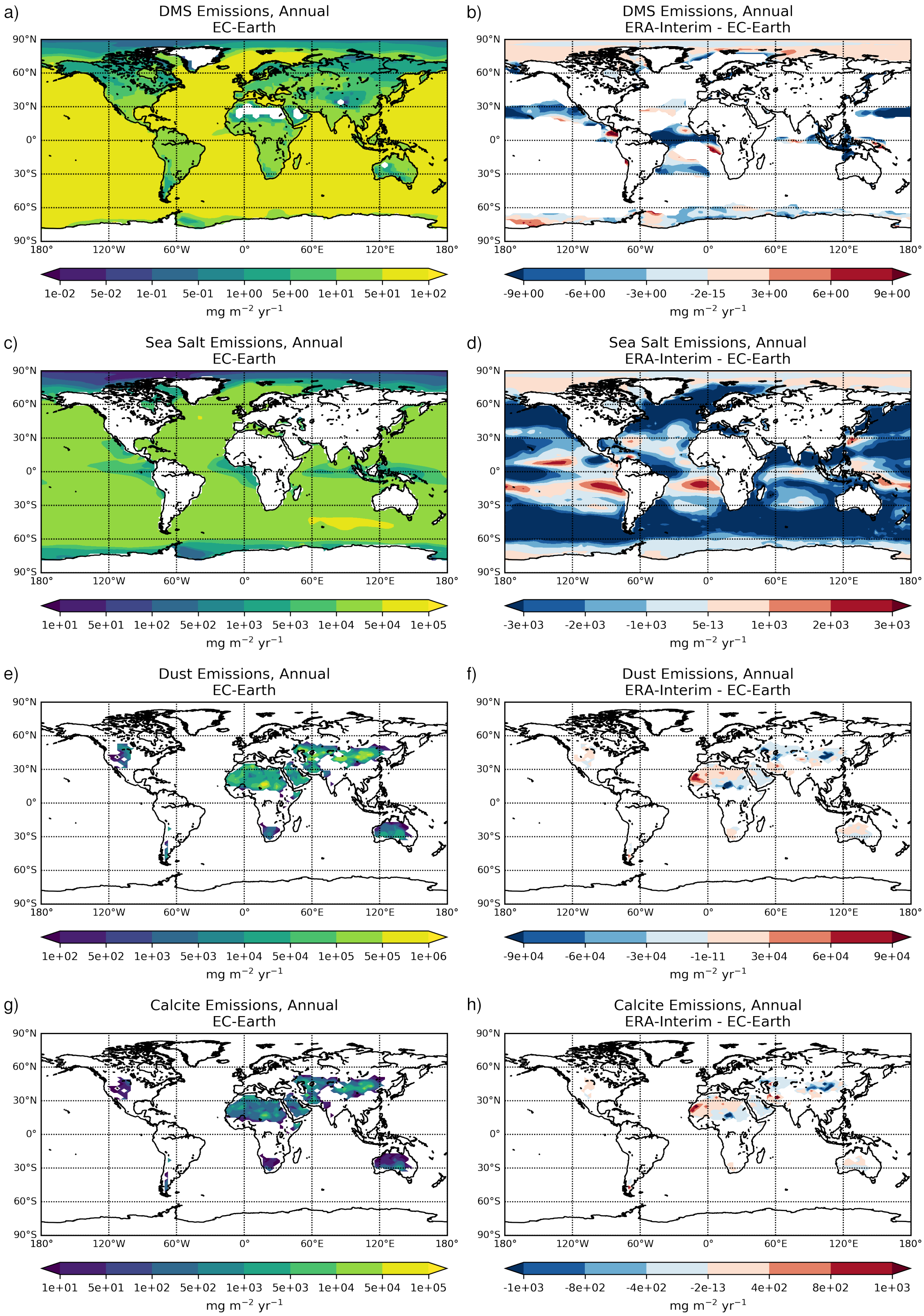

Figure S4: Annual mean emission fluxes (mg m^{-2} yr^{-1}) of a) DMS, c) sea salt, e) mineral dust, and g) calcite (in mg Ca m^{-2} yr^{-1}), as calculated for the EC-Earth simulation, averaged for the period 2000-2014, and the respective absolute differences to the ERA-Interim simulation (b,d,f,h).

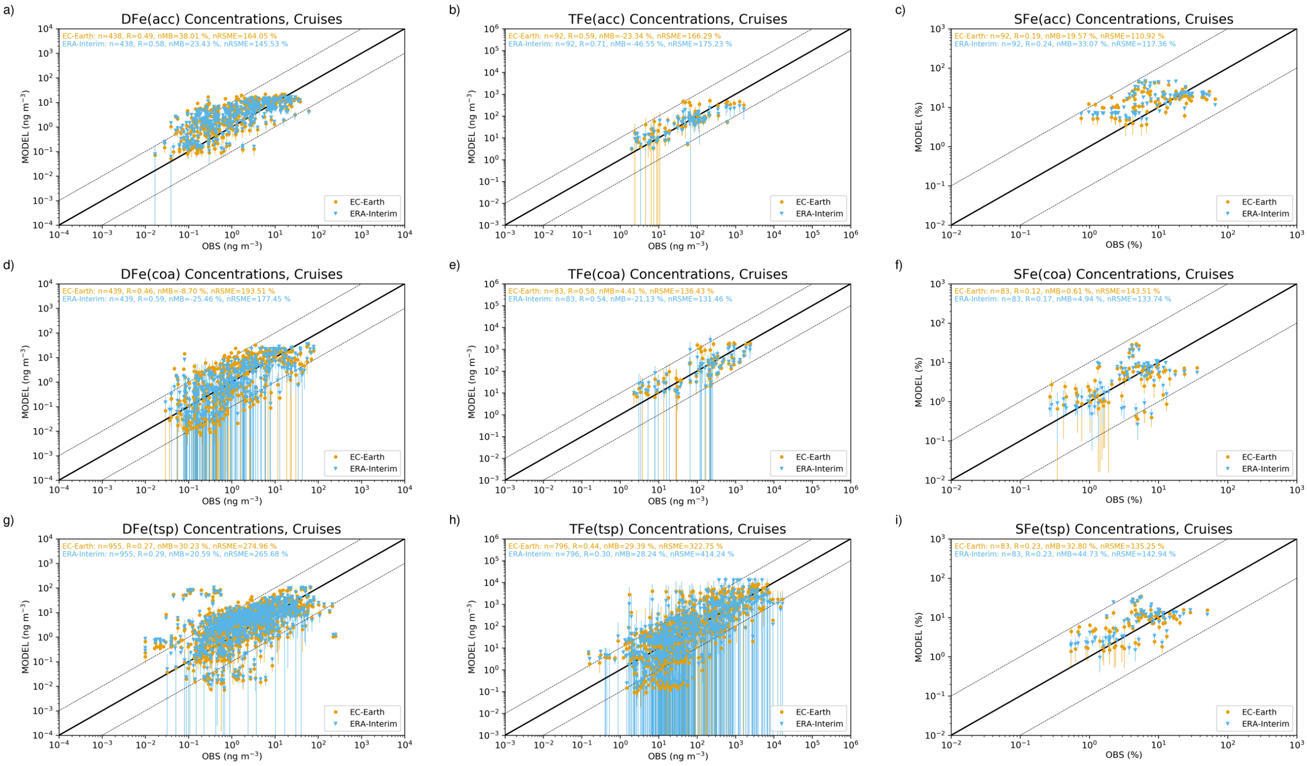

Figure S5: Scatterplot comparisons of cruise observations (see text) for accumulation aerosols (top), coarse aerosols (middle), and total suspended matter (bottom) of dissolved iron (DFe; a,d,g), total iron (TFe; b,e,h) aerosols (ng m^{-3}) and the derived aerosol solubility (SFe=%DFe/TFe; c,f,i) of EC-Earth (orange circles) and ERA-Interim (light blue triangles) simulations; the solid line represents the 1 : 1 correspondence and the dashed lines show the 10 : 1 and 1 : 10 relationships, respectively. The color-coded error bars represent the model's standard error of the multi-annual mean for the individual observational period. Summary statistics (color-coded) for all points are also included.

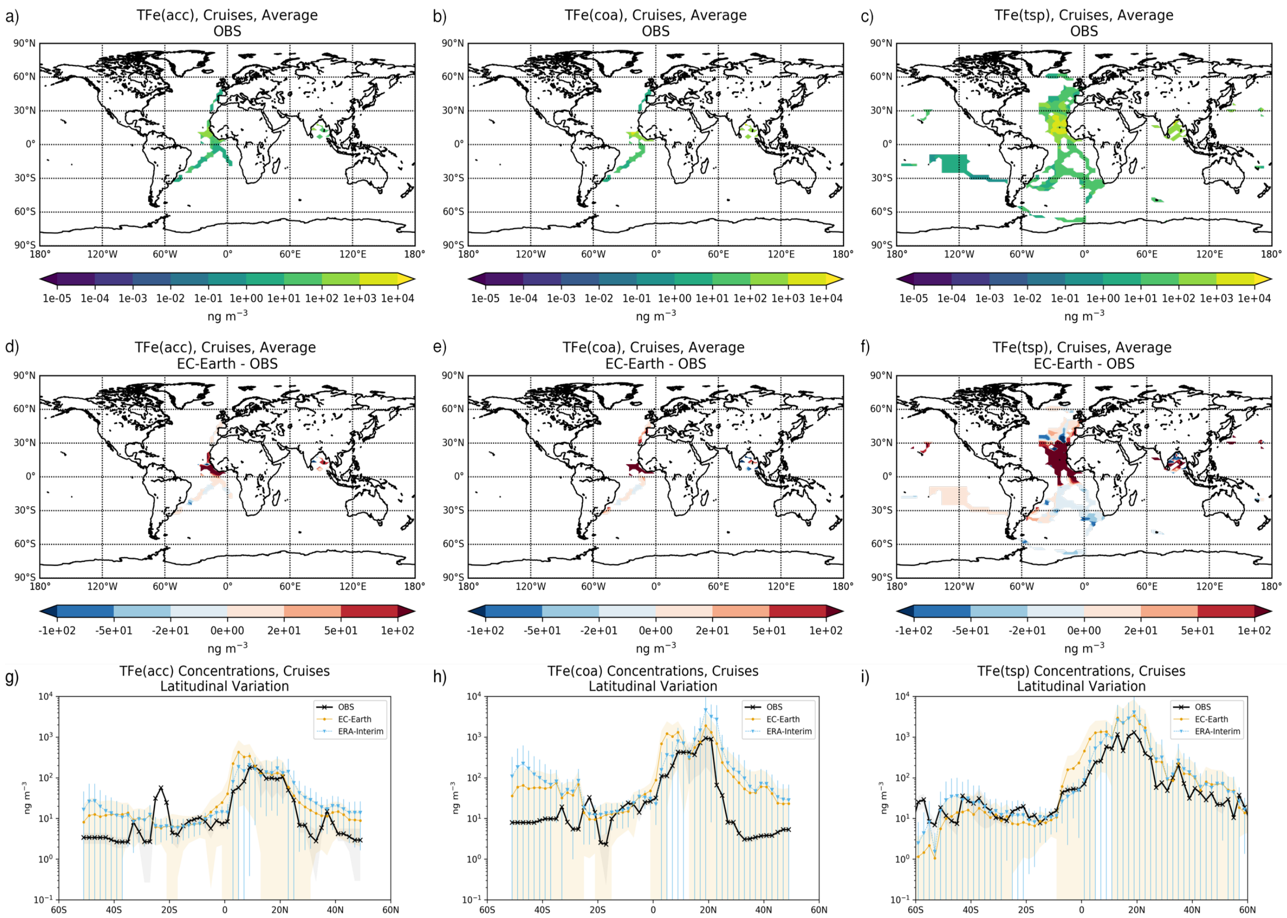

Figure S6: Observed total iron (TFe) concentrations (ng m^{-3}) of a) accumulation aerosols, b) coarse aerosols, and c) total suspended particles (tsp), the respective absolute differences to the ERA-Interim simulation (d,e,f), and the comparison to observations (black x-line) in latitudinal order (g,e,f) with the EC-Earth (orange circle-line) and ERA-Interim (light blue triangle-line) simulations; the grey shaded areas correspond to the standard deviation of the observations and the color-coded error bars/shaded areas correspond to the model's standard error of the multi-annual mean for the individual observational period.

References

Bibi, I., Singh, B. and Silvester, E.: Dissolution kinetics of soil clays in sulfuric acid solutions: Ionic strength and temperature effects, Appl. Geochemistry, 51, 170–183, doi:10.1016/j.apgeochem.2014.10.004, 2014.

Bonneville, S., Van Cappellen, P. and Behrends, T.: Microbial reduction of iron(III) oxyhydroxides: effects of mineral solubility and availability, Chem. Geol., 212(3), 255–268, doi:10.1016/j.chemgeo.2004.08.015, 2004.

Carlton, A. G., Turpin, B. J., Altieri, K. E., Seitzinger, S., Reff, A., Lim, H.-J. and Ervens, B.: Atmospheric oxalic acid and SOA production from glyoxal: Results of aqueous photooxidation experiments, Atmos. Environ., 41(35), 7588–7602, doi:10.1016/j.atmosenv.2007.05.035, 2007.

Claquin, T., Schulz, M. and Balkanski, Y. J.: Modeling the mineralogy of atmospheric dust sources, J. Geophys. Res. Atmos., 104(D18), 22243–22256, doi:10.1029/1999JD900416, 1999.

Deguillaume, L., Leriche, M., Monod, A. and Chaumerliac, N.: The role of transition metal ions on HO_x radicals in clouds: a numerical evaluation of its impact on multiphase chemistry, Atmos. Chem. Phys., 4(1), 95–110, doi:10.5194/acp-4-95-2004, 2004.

Deguillaume, L., Tilgner, A., Schrödner, R., Wolke, R., Chaumerliac, N. and Herrmann, H.: Towards an operational aqueous phase chemistry mechanism for regional chemistry-transport models: CAPRAM-RED and its application to the COSMO-MUSCAT model, J. Atmos. Chem., 64(1), 1–35, doi:10.1007/s10874-010-9168-8, 2009.

Deguillaume, L., Desboeufs, K. V., Leriche, M., Long, Y. and Chaumerliac, N.: Effect of iron dissolution on cloud chemistry: from laboratory measurements to model results, Atmos. Pollut. Res., 1(4), 220–228, doi:10.5094/APR.2010.029, 2010.

Ervens, B., George, C., Williams, J. E., Buxton, G. V., Salmon, G. A., Bydder, M., Wilkinson, F., Dentener, F., Mirabel, P., Wolke, R. and Herrmann, H.: CAPRAM 2.4 (MODAC mechanism): An extended and condensed tropospheric aqueous phase mechanism and its application, J. Geophys. Res., 108(D14), 4426, doi:10.1029/2002JD002202, 2003.

Ervens, B., Feingold, G., Frost, G. J. and Kreidenweis, S. M.: A modeling study of aqueous production of dicarboxylic acids: 1. Chemical pathways and speciated organic mass production, J. Geophys. Res., 109(D15), D15205, doi:10.1029/2003JD004387, 2004.

Herrmann, H., Ervens, B., Jacobi, H. W., Wolke, R., Nowacki, P. and Zellner, R.: CAPRAM2.3: A chemical aqueous phase radical mechanism for tropospheric chemistry, J. Atmos. Chem., 36(3), 231–284, doi:10.1023/A:1006318622743, 2000.

Herrmann, H., Tilgner, A., Barzaghi, P., Majdik, Z., Gligorovski, S., Poulain, L. and Monod, A.: Towards a more detailed description of tropospheric aqueous phase organic chemistry: CAPRAM 3.0, Atmos. Environ., 39(23–24), 4351–4363, doi:10.1016/j.atmosenv.2005.02.016, 2005.

Hoesly, R. M., Smith, S. J., Feng, L., Klimont, Z., Janssens-Maenhout, G., Pitkanen, T., Seibert, J. J., Vu, L., Andres, R. J., Bolt, R. M., Bond, T. C., Dawidowski, L., Kholod, N., Kurokawa, J., Li, M., Liu, L., Lu, Z., Moura, M. C. P., O Rourke, P. R. and Zhang, Q.: Historical (1750–2014) anthropogenic emissions of reactive gases and aerosols from the Community Emissions Data System (CEDS), Geosci. Model Dev., 11(1), 369–408, doi:10.5194/gmd-11-369-2018, 2018.

Ito, A.: Atmospheric Processing of Combustion Aerosols as a Source of Bioavailable Iron, Environ. Sci. Technol. Lett., 2(3), 70–75, doi:10.1021/acs.estlett.5b00007, 2015.

Ito, A. and Shi, Z.: Delivery of anthropogenic bioavailable iron from mineral dust and combustion aerosols to the ocean, Atmos. Chem. Phys., 16(1), 85–99, doi:10.5194/acp-16-85-2016, 2016.

Ito, A., Lin, G. and Penner, J. E.: Radiative forcing by light-absorbing aerosols of pyrogenetic iron oxides, Sci. Rep., 8(1), 7347, doi:10.1038/s41598-018-25756-3, 2018.

Lim, H.-J., Carlton, A. G. and Turpin, B. J.: Isoprene Forms Secondary Organic Aerosol through Cloud Processing: Model Simulations, Environ. Sci. Technol., 39(12), 4441–4446, doi:10.1021/es048039h, 2005.

Lin, G., Sillman, S., Penner, J. E. and Ito, A.: Global modeling of SOA: the use of different mechanisms for aqueous-phase formation, Atmos. Chem. Phys., 14(11), 5451–5475, doi:10.5194/acp-14-5451-2014, 2014.

van Marle, M. J. E., Kloster, S., Magi, B. I., Marlon, J. R., Daniau, A.-L., Field, R. D., Arneth, A., Forrest, M., Hantson, S., Kehrwald, N. M., Knorr, W., Lasslop, G., Li, F., Mangeon, S., Yue, C., Kaiser, J. W. and van der Werf, G. R.: Historic global biomass burning emissions for CMIP6 (BB4CMIP) based on merging satellite observations with proxies and fire models (1750–2015), Geosci. Model Dev., 10(9), 3329–3357, doi:10.5194/gmd-10-3329-2017, 2017.

Sander, R.: Compilation of Henry's law constants (version 4.0) for water as solvent, Atmos. Chem. Phys., 15(8), 4399–4981, doi:10.5194/acp-15-4399-2015, 2015.

Sedlak, D. L. and Hoigné, J.: The role of copper and oxalate in the redox cycling of iron in atmospheric waters, Atmos. Environ. Part A, Gen. Top., 27(14), 2173–2185, doi:10.1016/0960-1686(93)90047-3, 1993.

Seinfeld, J. H. and Pandis, S. N.: Atmospheric Chemistry and Physics: From Air Pollution to Climate Change., 2006.

Shi, Z., Krom, M. D., Bonneville, S., Baker, A. R., Jickells, T. D. and Benning, L. G.: Formation of Iron Nanoparticles and Increase in Iron Reactivity in Mineral Dust during Simulated Cloud Processing, Environ. Sci. Technol., 43(17), 6592–6596, doi:10.1021/es901294g, 2009.

Shi, Z., Krom, M. D., Bonneville, S. and Benning, L. G.: Atmospheric Processing Outside Clouds Increases Soluble Iron in Mineral Dust, Environ. Sci. Technol., 49(3), 1472–1477, doi:10.1021/es504623x, 2015.

Tan, Y., Lim, Y. B., Altieri, K. E., Seitzinger, S. P. and Turpin, B. J.: Mechanisms leading to oligomers and SOA through aqueous photooxidation: insights from OH radical oxidation of acetic acid and methylglyoxal, Atmos. Chem. Phys., 12(2), 801–813, doi:10.5194/acp-12-801-2012, 2012.